

Al₂₂Cl₂₀·12L (L = THF, THP): The First Polyhedral Aluminum Chlorides

Christoph Klemp,[†] Michael Bruns,[‡] Jürgen Gauss,[§] Ulrich Häussermann,^{||} Gregor Stösser,[†] Leo van Wüllen,[⊥] Martin Jansen,[⊥] and Hansgeorg Schnöckel^{*,†}

Contribution from the Institut für Anorganische Chemie der Universität Karlsruhe (TH), Engesserstrasse Gebäude 30.45, D-76128 Karlsruhe, Germany, Forschungszentrum Karlsruhe, Institut für Instrumentelle Analytik, Hermann-von-Helmholtz-Platz 1, D-76344 Eggenstein-Leopoldshafen, Germany, Institut für Physikalische Chemie, Universität Mainz, D-55099 Mainz, Germany, Inorganic Chemistry, Stockholm University, Stockholm, Sweden, and Max-Planck-Institut für Festkörperforschung, Stuttgart, Germany

Received November 20, 2000

Abstract: Aluminum subhalides of the type Al₂₂X₂₀·12L (X = Cl, Br; L = THF, THP) are the only known representatives of polyhedral aluminum subhalides and exhibit interesting multicenter bonding properties. Herein, we report on the synthesis and structural investigation of the first chlorides of this type. Additional investigations applying solid-state ²⁷Al NMR (MAS), XPS (of Al₄Cp*₄ and Al₂₂X₂₀·12L), and quantum chemical calculations shed more light upon the structure of the molecules and possible Al modifications.

Introduction

Subhalides of all group XIII elements E_nX_m (E = triels B, Al, Ga, In, Tl; X = F, Cl, Br, I) are now well known. These compounds offer a great variety of structures which extend from the well-known saltlike Tl(I) halides to the molecular polyhedral boron subhalides such as, for example, B₄X₄ and B₈X₈.¹ The subhalides of the elements Al, Ga, and In prefer the composition E_nX_{n+2} with n = 2, e.g., in compounds of the type L·X₂E–EX₂·L (L = donor).² Mixed-valent species, which were previously known for the element boron, were recently also found for Al and Ga (n = 3 or 5).³ It even proved possible to isolate (oligomeric) monohalides of the E_nX_n type (E = Al, Ga), i.e., Ga₈I₈·6NET₃ and Al₄X₄·4L (X = Br, I; L = NET₃, PET₃),⁴ from donor-stabilized metastable EX solutions obtained by co-condensation.⁵ Owing to the strong electron donors used, discrete 2e[−]–2c bonds are formed, thus yielding ring structures instead of E_nX_n polyhedra known from boron compounds.⁶

* Corresponding author: (fax) +49 (721) 608-4854; (e-mail) hg@achpc9.chemie.uni-karlsruhe.de.

[†] Institut für Anorganische Chemie der Universität Karlsruhe.

[‡] Institut für Instrumentelle Analytik.

[§] Universität Mainz.

^{||} Stockholm University.

[⊥] Max-Planck-Institut für Festkörperforschung.

(1) (a) {B₉X₉}: Hönle, W.; Grin, Y.; Burkhardt, A.; Wedig, U.; Schultheiss, M.; Schnering, H. G. v.; Keller, R.; Binder, H. *J. Solid State Chem.* **1997**, *133*, 59. (b) {B₆I₆[−], B₆I₆^{2−}}: Heinrich, A.; Keller, H.-L.; Preetz, W. *Z. Naturforsch. B* **1990**, *45*, 184.

(2) (a) {Al₂X₄·2L}: Ecker, A.; Friesen, M. A.; Junker, M. A.; Üffing, C.; Köppe, R.; Schnöckel, H. *Z. Anorg. Allg. Chem.* **1998**, *624*, 513. Mocker, M.; Robl, C.; Schnöckel, H. *Angew. Chem.* **1994**, *106*, 946; *Angew. Chem., Int. Ed. Engl.* **1994**, *33*, 862. (b) {Ga₂X₄·2L}: Beagley, B.; Godfrey, S.; Kelly, K.; Kungwankunakorn, S.; McAuliffe, C.; Pritchard, R. *Chem. Commun.* **1996**, 2179. Beamish, J. C.; Boardman, A.; Small, R. W. H.; Worrall, I. J. *Polyhedron* **1985**, *4*, 983. Beamish, J. C.; Small, R. W. H.; Worrall, I. J. *Inorg. Chem.* **1979**, *18*, 220. Small, R. W. H.; Worrall, I. J. *Acta Crystallogr.* **1982**, *38b*, 250.

(3) (a) {Ga₃I₅·3PET₃}: Schnepf, A.; Doriat, C.; Möllhausen, E.; Schnöckel, H. *Chem. Commun.* **1997**, 2111. (b) {Ga₅Cl₇·5THF}: Loos, D.; Schnöckel, H.; Fenske, D. *Angew. Chem.* **1993**, *105*, 1124; *Angew. Chem., Int. Ed. Engl.* **1993**, *32*, 1059. (c) {Al₃Br₇·5THF}: Klemp, C.; Stösser, G.; Krossing, I.; Schnöckel, H. *Angew. Chem.* **2000**, *112*, 3834; *Angew. Chem., Int. Ed. Engl.* **2000**, *39*, 3691.

Whereas no example of a polyhedral gallium subhalide is known, we have recently characterized the first polyhedral aluminum subhalide, namely, Al₂₂Br₂₀·12THF (**1**).⁷ Herein, the first analogous chlorides Al₂₂Cl₂₀·12THF (**2**) and Al₂₂Cl₂₀·12THP (**3**) are described. The E_nX_{n−2}-type species **1**, **2**, and **3** represent the first examples for *metal-rich* clusters of triel subhalides.⁸ The properties of **2** and **3** were investigated using MAS and XPS.

Experimental Section

Synthesis of 2 and 3. Gaseous AlCl₃ was continuously produced by the high-temperature reaction between liquid Al and gaseous HCl at 1000 °C and 10^{−3} mbar. According to the established synthesis,⁵ metastable AlCl solutions were generated by co-condensation of 40 mmol of AlCl together with 85 mL of toluene and 15 mL of either THF or THP. A 100-mL sample of donor-stabilized 0.4 M AlCl solutions is obtained in this way.

Typically 10 mL of these dark red solutions was concentrated to half volume at room temperature, thereby removing the excess of donor solvent. Within several hours, small quantities of aluminum precipitated. After a few days, from the further concentrated filtrate pale yellow hexagonal plates of **2** respective to **3** crystallized. Yield: 47 mg (0.021 mmol, 11.5%) for **2** and 13 mg (0.054 mmol, 3%) for **3**.

The crystals were not soluble but decomposed on dissolution to yield AlX₃ and further byproducts which were not yet characterized. They

(4) (a) {Ga₈I₈·6NET₃}: Doriat, C.; Friesen, M.; Baum, E.; Ecker, A.; Schnöckel, H. *Angew. Chem.* **1997**, *109*, 2057; *Angew. Chem., Int. Ed. Engl.* **1997**, *36*, 1969. (b) {Al₄Br₄·4NET₃}: Mocker, M.; Robl, C.; Schnöckel, H. *Angew. Chem.* **1994**, *106*, 1860; *Angew. Chem., Int. Ed. Engl.* **1994**, *33*, 1754. (c) {Al₄I₄·4D}: Ecker, A.; Schnöckel, H. *Z. Anorg. Allg. Chem.* **1998**, *624*, 813.

(5) Dohmeier, C.; Loos, D.; Schnöckel, H. *Angew. Chem.* **1996**, *108*, 141; *Angew. Chem., Int. Ed. Engl.* **1996**, *35*, 129.

(6) For B₄X₄ compounds, however, Libscomb postulated a planar tetrameric structure as an intermediate in the ("diamond–square–diamond") isomerization of these compounds.^{41a} Furthermore, there also exist anionic polyhedral boron compounds like B₁₂F₁₂^{2−}.^{41b}

(7) Klemp, C.; Köppe, R.; Weckert, E.; Schnöckel, H. *Angew. Chem.* **1999**, *111*, 1851; *Angew. Chem., Int. Ed. Engl.* **1999**, *38*, 1739.

(8) To our knowledge, the Al₂₂X₂₀·12L compound is in fact the only example at all of a neutral molecular icosahedral M₁₂ cluster compound outside the boron chemistry.

are mechanically unstable, sensitive to air or moisture, and powder in vacuo. Suitable single crystals for X-ray structure analysis as well as for NMR and XPS investigations were obtained from several similar experiments.

X-ray Crystallography. The single crystals decomposed in dry perfluoropolyether oil within a few minutes. Therefore, they were mounted quickly after adding them together with the concentrated AlCl solution to the perfluoropolyether oil which was cooled to $-20\text{ }^{\circ}\text{C}$. X-ray diffraction data were collected on a STOE IPDS diffractometer with graphite-monochromatized Mo K α radiation ($\lambda = 0.710\text{ }73\text{ \AA}$) at 190 K. The structures were solved by direct methods (Shelxs 97). A total of 534 and 611 parameters for **2** and **3**, respectively, were refined by full-matrix least squares against F^2 (Shelxl 97) with anisotropic thermal parameters for all non-hydrogen atoms. H atoms were refined on calculated positions according to the riding model. **2** and **3** contain four slightly disordered toluene molecules per Al₂₂ unit. Furthermore, some of the C atoms of the donor molecules and two Cl atoms are slightly disordered.⁹

Mass Spectrometry. Mass spectrometric investigations were carried out on Varian MAT 711 and Finnigan MAT MS8223 spectrometers, EI = 70 eV; DI = 50–150 $^{\circ}\text{C}$. The observed masses and isotopic patterns were in good agreement with the calculated values.

NMR Investigations. MAS and MQMAS experiments were carried out at 9.4-T using a Bruker DSSX400 NMR spectrometer, equipped with a 2.5-mm MAS probe, employing MAS frequencies of 30 kHz and rf amplitudes of 170 kHz. Chemical shifts were referenced relative to 1 M aqueous Al(NO₃)₃. A non-rotor-synchronized, z -filtered 3QMAS pulse sequence¹⁰ was used for the ²⁷Al MQMAS experiment.

XPS Investigations. The XPS data were acquired using an Escalab 5 multimethod spectrometer (Vacuum Generators, East Grinstead, U.K.) with a nonmonochromatized Mg K α X-ray source (1253.6 eV) operating at 200 W. The sample area was $\sim 50\text{ mm}^2$. The kinetic energies of the photoelectrons were measured with a hemispheric 150 $^{\circ}$ sector field analyzer in CAE mode (constant analyzer energy) with a pass energy of 20 eV for narrow scans. The binding energy (BE) scale was calibrated with the known photoelectron energies of Au, Ag, and Cu (fwhm = 1.2 eV for Au 4f_{7/2} = 84.0 eV).

Spectrometer controlling and data collecting were conducted with the software package VGX-900 (VG Microtech); data analysis was performed by peak fitting, employing the program UNIFIT FÜR WINDOWS (University of Leipzig).¹¹ The BE reference was set to 285.0 eV for C 1s of alkyl carbon. Due to differential charging,^{12a} the accuracy of the determined BE is at least 0.3 eV with a fwhm between 2.0 and 2.5 eV. We found a BE for Al 2p of 72.5 eV for a freshly sputtered Al foil. The Al 2p doublet was not separated. Shirley background correction^{12b} was applied.

A 10-mg sample of single crystals was washed with dry pentane and transferred with the help of an argon glovebox. Clean sample

(9) Crystallographic data for **2**: C₉₀H₁₄₄Al₂₂Cl₂₀O₁₂, 2720.61 g·mol⁻¹, pale yellow plate $0.3 \times 0.2 \times 0.1\text{ mm}^{-3}$, triclinic $P\bar{1}$ (No. 2), $a = 15.806(3)\text{ \AA}$, $b = 16.530(3)\text{ \AA}$, $c = 16.669(3)\text{ \AA}$, $\alpha = 69.95(3)^{\circ}$, $\beta = 61.88(3)^{\circ}$, $\gamma = 84.97(3)^{\circ}$, $V = 3594.0(12)\text{ \AA}^3$, and $Z = 1$, $\rho_{\text{ber}} = 1.257\text{ Mg}\cdot\text{m}^{-3}$, $\mu_{\text{Mo}} = 0.56\text{ mm}^{-1}$, $\theta_{\text{min}} = 0.7415^{\circ}$, $\theta_{\text{max}} = 0.8501^{\circ}$; reflections, 27 844 measured, 12 949 unique ($R_{\text{int}} = 0.1062$), 6065 $F > 4\sigma(F)$, numerical absorption correction (min/max transmission: 0.7415/0.8501), $\text{gof} = 0.922$, 534 parameters, $R_1(>4\sigma) = 0.0968$, $wR_2 = 0.2891$; remaining electron density, max 0.686 e·Å⁻³, min $-0.549\text{ e}\cdot\text{\AA}^{-3}$. Crystallographic data for **3**: C₁₀₂H₁₂₀Al₂₂Cl₂₀O₁₂, 2840.54 g·mol⁻¹, pale yellow plate $0.3 \times 0.1 \times 0.05\text{ mm}^{-3}$, triclinic $P\bar{1}$ (No. 2), $a = 15.060(3)\text{ \AA}$, $b = 15.768(3)\text{ \AA}$, $c = 18.190(4)\text{ \AA}$, $\alpha = 96.78(3)^{\circ}$, $\beta = 105.91(3)^{\circ}$, $\gamma = 111.38(3)^{\circ}$, $V = 3751.4(13)\text{ \AA}^3$, and $Z = 1$, $\rho_{\text{ber}} = 1.257\text{ Mg}\cdot\text{m}^{-3}$, $\mu_{\text{Mo}} = 0.539\text{ mm}^{-1}$, $\theta_{\text{min}} = 0.6553^{\circ}$, $\theta_{\text{max}} = 0.7511^{\circ}$; reflections, 21 687 measured, 11 149 unique ($R_{\text{int}} = 0.1046$), 4104 $F > 4\sigma(F)$, numerical absorption correction (min/max transmission, 0.6553/0.7511), $\text{gof} = 0.798$, 611 parameters, $R_1(>4\sigma) = 0.0721$, $wR_2 = 0.1929$; remaining electron density, max 0.549 e·Å⁻³, min $-0.342\text{ e}\cdot\text{\AA}^{-3}$.

(10) Amoureux, J.-P.; Fernandez, C.; Steuernagel, S. *J. Magn. Reson.* **1996**, *123*, 116.

(11) Hesse, R. *Research Report UNIFIT 2.1*, University of Leipzig, Germany, 1998.

(12) (a) Gross, Th.; Lippitz, A.; Unger, W. E. S.; Lehnert, A.; Schmid, G. *Appl. Surf. Sci.* **1994**, *345*. (b) Briggs, D., Seah, M. P., Ed. *Practical Surface Analysis by Auger and X-ray Photoelectron Spectroscopy*, 2nd ed.; Wiley & Sons: Chichester, U.K., 1990.

surfaces were produced by crushing single crystals in the ultrahigh-vacuum recipient (basic pressure $< 10^{-10}$ mbar). All samples were measured at 78 K in order to reduce the risk of sample decomposition, which occurred even at that temperature during several hours (cf. Supporting Information).

Quantum Chemical Calculations. The structures for the model systems Al₁₂[AlCl₂·H₂O]₁₀ (S_5 symmetry) (**2a**), Al₁₂[AlCl₂·THF]₁₀·2THF (C_i) (**2b**), [AlCl₂·H₂O]₂ (D_{2h}), AlCl₃·H₂O (C_i), and AlCl₃·2H₂O (C_i) were optimized at the density functional theory (DFT) level¹³ employing the Becke–Perdew (BP86) functional¹⁴ together with an auxiliary basis approximation for the Coulomb energy (RI-DFT).¹⁵ A polarized split-valence basis (SV(P))¹⁶ was used, where the parentheses indicate that polarization functions were only considered for non-hydrogen atoms.

The ²⁷Al NMR chemical shifts for **2b** were computed by employing the gauge-including atomic orbital (GIAO) Hartree–Fock self-consistent-field (HF-SCF) method^{17,18} using a double- ζ polarization (DZP) basis¹⁶ for Al and Cl and the SV(P) basis¹⁶ for the THF ligands. Relative shifts were obtained with AlH₄⁻ as internal reference and a $\delta^{27}\text{Al}$ value for AlH₄⁻ of 101 ppm (the absolute shielding calculated for AlH₄⁻ at the GIAO-HF-SCF/DZP level is 517.1 ppm).¹⁹

Nuclear quadrupole coupling tensors were obtained for **2b** using the following expressions²⁰

$$\chi_{ab} = eQq_{ab}/h$$

where e is the elementary charge, Q is the nuclear quadrupole moment, h is Planck's constant, and q_{ab} is the electric field gradient at the corresponding nuclear positions. The latter were obtained from HF-SCF calculations using a polarized triple- ζ (TZP) basis¹⁶ for Al and Cl and SV(P) for the remainder of the molecule. The value for nuclear quadrupole moment of ²⁷Al was taken from ref 21. As usual, the quadrupole coupling constant CQ and the asymmetry factor η are reported.

$$CQ = \chi_{zz}$$

$$\eta = (\chi_{xx} - \chi_{yy})/\chi_{zz}$$

where χ_{zz} , χ_{yy} , and χ_{xx} are the diagonal elements of the quadrupole coupling tensor in the principal axis system. The latter are by convention ordered as $|\chi_{zz}| \geq |\chi_{yy}| \geq |\chi_{xx}|$.

For all calculations, the TURBOMOLE program package was used.²²

The quantum chemical calculations on solid aluminum (assuming crystal structures of the cubic close packing (fcc) and α -rhombohedral boron) were performed using the full-potential linearized augmented plane wave (FLAPW) method of the WIEN program package.²³ Well-converged plane wave basis sets with a cutoff parameter $R_{\text{mt}}K_{\text{max}} = 8.0$ and 816 (fcc) and 44 (α -B) K points in the irreducible wedges of the corresponding Brillouin zones were used. The LDA exchange correlation potential was parametrized according to Perdew and Wang.²⁴

(13) See, for example: Parr, R. G.; Yang, W. *Density-Functional Theory of Atoms and Molecules*; Oxford University Press: New York, 1989.

(14) Becke, A. D. *Phys. Rev. A* **1998**, *38*, 3098. Perdew, J. P. *Phys. Rev. B* **1996**, *33*, 8822.

(15) Eichkorn, K.; Treutler, O.; Öhm, H.; Häser, M.; Ahlrichs, R. *Chem Phys. Lett.* **1995**, *240*, 283.

(16) Schäfer, A.; Horn, H.; Ahlrichs, R. *J. Chem. Phys.* **1992**, *97*, 2571.

(17) Wolinski, K.; Hinton, J. F.; Pulay, P. *J. Am. Chem. Soc.* **1990**, *112*, 8251.

(18) Häser, M.; Ahlrichs, R.; Baron, H. P.; Weis, P.; Horn, H. *Theor. Chim. Acta* **1992**, *83*, 455.

(19) Nöth, H. *Z. Naturforsch. B* **1980**, *35*, 119 and references therein.

(20) See, for example: Abragam, A. *Principles of Nuclear Magnetism*; Oxford University Press: Oxford, U.K., 1961.

(21) Mills, I.; Cvitas, T.; Homann, K.; Kallay, N.; Kuchitsu, K. *Quantities, Units and Symbols in Physical Chemistry*; Blackwell Science: Oxford, U.K., 1993.

(22) Ahlrichs, R.; Bär, M.; Häser, M.; Horn, H.; Kölmel, C. *Chem. Phys. Lett.* **1989**, *162*, 165.

(23) Blaha, P.; Schwarz, K.; Luitz, J. *Program WIEN97: A Full Potential Linearized Augmented Plane Wave Package for Calculating Crystal Properties*; Schwarz, K.; Techn. Universität Wien, Austria, 1999.

(24) Perdew, J. P.; Wang, Y. *Phys. Rev. B* **1992**, *45*, 13244.

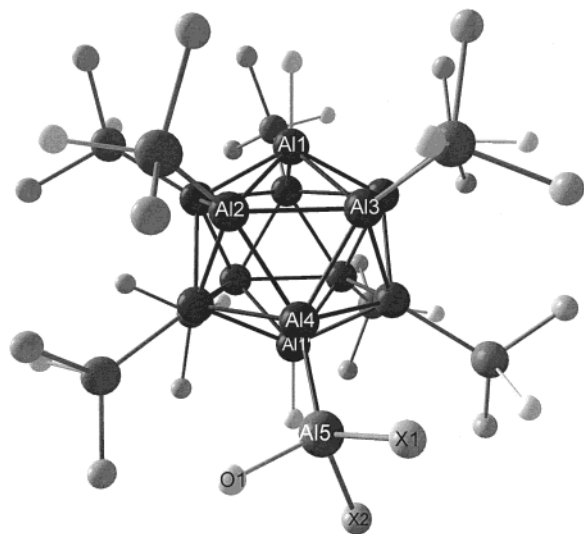


Figure 1. Molecular structure of **3** within the crystal (exemplary for **1**, **2**, and **3**). C and H atoms are omitted for clarity. The numbering of Al atoms refers to the three different kinds of Al atoms (Al1, Al2–4, Al5).

Table 1. Averaged Al Distances (Å) of **2** and **3** in Comparison to **1** and Calculated Values for **2a** and **2b** (Numbers According to Figure 1)

	2	3	1	2a	2b
Al1–Al2	2.649	2.652	2.650	2.615	2.656
Al2–Al3	2.763	2.762	2.762	2.824	2.775
Al3–Al4	2.692	2.691	2.692	2.684	2.695
Al4–Al5	2.549	2.552	2.526	2.541	2.563
Al5–X	2.173	2.171	2.299	2.211	2.212
Al–O	1.875	1.884	1.892	1.937	1.950

Results and Discussion

The co-condensation of AlCl_3 with toluene and either tetrahydrofuran (THF) or tetrahydropyran (THP) as a donor resulted in both cases in metastable dark red solutions from which aluminum precipitated at room temperature. From the concentrated filtrates, very sensitive pale yellow crystals of $\text{Al}_{12}\text{Cl}_{20} \cdot 12\text{THF}$ (**2**) respective of $\text{Al}_{12}\text{Cl}_{20} \cdot 12\text{THP}$ (**3**) were isolated.

Molecular Structure. The molecular structures of **2** and **3** as established by X-ray structural analysis⁹ are similar to the bromide **1**.⁷ Figure 1 shows as an example the structure of **3**. The Al atoms are numbered according to three different chemical environments (Al1, Al2–4, Al5) and not for crystallographic reasons.

DFT calculations conducted on the model systems $\text{Al}_{12}\text{Cl}_{20} \cdot 10\text{H}_2\text{O}$ (**2a**) and $\text{Al}_{12}\text{Cl}_{20} \cdot 12\text{THF}$ (**2b**) show great conformity with this geometry. The results will be discussed below. The Al–Al distances of **1**, **2**, and **3** are nearly identical and fall into the range expected for subvalent Al compounds. In Table 1 they are compared to the corresponding values calculated for **2a** and **2b**.

A compressed Al_{12} icosahedron surrounded by 10 $\text{AlCl}_2 \cdot \text{L}$ ligands is found as the central unit. The compound can therefore be identified as $\text{Al}_{12}[\text{AlCl}_2 \cdot \text{L}]_{10} \cdot 2\text{L}$. Two Al atoms in the para position of the icosahedron (Al1 and Al1') are not bonded to an $\text{AlCl}_2 \cdot \text{L}$ unit but coordinated by a donor molecule instead. In this direction, the diameter of the icosahedron is 4.70 Å, which is ~10% shorter compared to the other directions (5.20 ± 0.02 Å). The 20 chlorine atoms adopt the geometry of a distorted pentagonal dodecahedron with a donor molecule protruding out of each pentagonal plane. Figure 2 shows the space filling model of **3** and the complete coverage of the

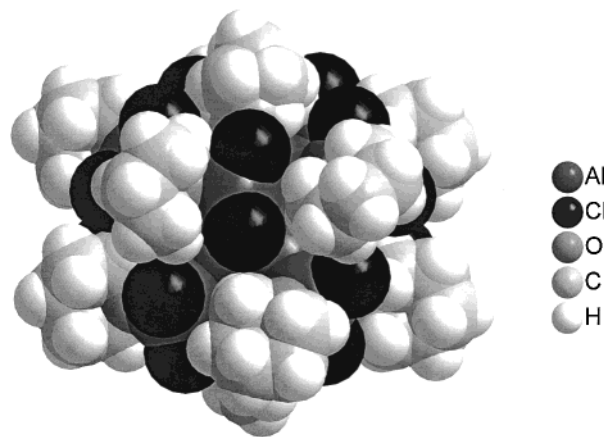


Figure 2. Space filling model of **3**. The subvalent Al atoms are completely covered by a closed shell of Cl atoms (pentagonal dodecahedral arrangement) and methylene groups of the donor molecules (icosahedral arrangement).

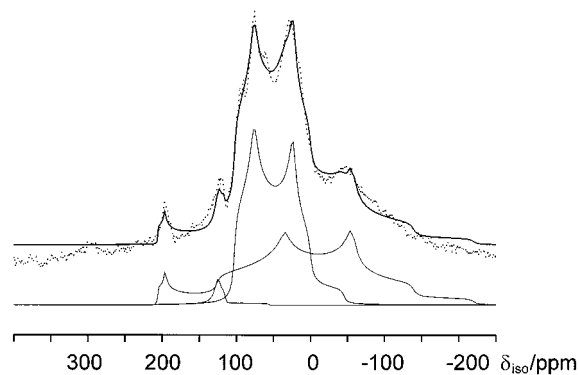


Figure 3. ^{27}Al MAS spectra for **1** (single-pulse excitation). Dotted line, experimental spectrum; solid line, simulation of the spectrum assuming three individual quadrupolar powder patterns (below the spectrum) using the parameters given in Table 4.

subvalent Al atoms by a closed shell of Cl atoms and methylene groups of the donor molecules.

Mass Spectrometry. In our experiments, these compounds turned out to be very unstable. Upon heating above 100 °C, the crystals decompose to give $\text{AlCl}_3 \cdot \text{THF}$ and aluminum, and therefore, the mass spectrum of **2** does not show the molecular peak. The dominating fragment is $[\text{AlCl}_2 \cdot \text{THF}]^+$ ($m/z = 169$) (above DI = 50 °C). This result is in agreement to the previously observed formation of $[\text{AlBr}_2 \cdot \text{THF}]^+$ ($m/z = 258.9$) in the case of **1** (above DI = 70 °C). In terms of chemical reactions, these $\text{AlX}_2 \cdot \text{L}$ ligands probably represent ideal nucleofuges, as they can dimerize forming $\text{Al}_2\text{X}_4 \cdot 2\text{L}$.

NMR Investigations. Since the structures of the $\text{Al}_{12}[\text{AlX}_2 \cdot \text{L}]_{10} \cdot 2\text{L}$ polyhedra deviate from the ideal icosahedral symmetry, three distinctively different sets of Al atoms are expected in the ^{27}Al NMR spectrum. The NMR experiment has to be carried out in the solid state, because **1**, **2**, and **3** are insoluble without decomposition. The ^{27}Al magic angle spinning (MAS) NMR single-pulse excitation spectra for **1** and **2** are shown in Figures 3 and 4, respectively.

A broad signal was observed as the superposition of several, very broad powder patterns. The widths of the individual patterns reflect the expected very large quadrupolar coupling constants CQ, due to the highly asymmetric environment of the three different Al sites. To resolve the individual components, multiple quantum (MQ) MAS spectroscopy was used as

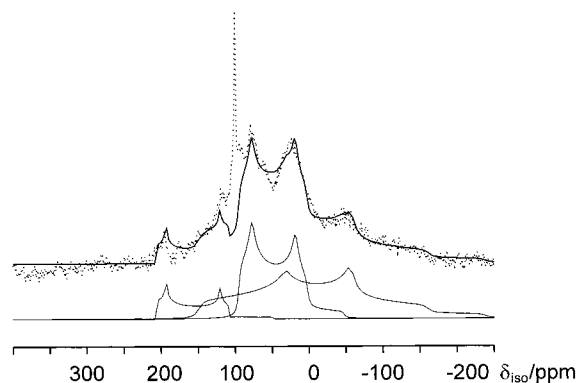


Figure 4. ^{27}Al MAS spectra for **2** (single-pulse excitation). Dotted line, experimental spectrum; solid line, simulation of the spectrum assuming three individual quadrupolar powder patterns (below the spectrum) using the parameters given in Table 4.

described 1995 by Frydman and co-workers.²⁵ In this method, the evolution of a multiple quantum coherence ($m \rightarrow -m$) is correlated with the evolution of a single quantum coherence under the conditions of fast MAS. In a 2D experiment, the projection on the F1 axis yields a highly resolved, isotropic spectrum, whereas the slices parallel to F2 represent the quadrupolar powder pattern.

Figure 5 shows the ^{27}Al MQMAS spectrum, obtained utilizing the coherence pathway $(0, \pm 3, 0, -1)$ (z -filtered 3QMAS¹⁰). Three different groups of signals can be identified in the isotropic projection on the F1 axis: (a) two signals at 126 and 142 ppm, (b) two signals at 198 and 208 ppm, and (c) one signal at 258 ppm.

The peaks labeled with an asterisk (*) belong to spinning side bands. Slices taken at these values in F1, parallel to the F2 axis, are plotted on the right-hand side in Figure 5. The chemical shifts in the F1 (MQ) dimension and the centers of gravity for the corresponding quadrupolar powder patterns (slices parallel F2) can now be used to extract the isotropic chemical shift δ_{iso} as well as the second-order quadrupolar effect SOQE, given by

$$\text{SOQE} = \text{CQ}(1 + \eta^2/3)^{1/2}$$

according to

$$\delta_{\text{iso}} = \delta_{\text{F2}} + (\delta_{\text{F1}} - \delta_{\text{F2}})17/27$$

and

$$\text{SOQE} = [(\delta_{\text{F1}} - \delta_{\text{iso}})(17/3)\{4S(2S - 1)^2 / \{4S(S + 1) - 3\}10^{-6}\nu_0^2\}^{1/2}]$$

where S is the nuclear spin, ν_0 the Larmor frequency, and η the asymmetry parameter. The resulting values are summarized in Table 2.

No δ_{iso} values could be extracted for the signals in group b, since the corresponding quadrupolar powder pattern exhibits a very poor signal-to-noise ratio due to an incomplete excitation of this site.²⁶ All we can state is that these Al sites must have an extremely large quadrupolar coupling constant.

(25) MQMAS: (a) Medek, A.; Harwood, J. S.; Frydman, L. *J. Am. Chem. Soc.* **1995**, *117*, 12779. (b) Medek, A.; Frydman, L. *J. Braz. Chem. Soc.* **1999**, *10*, 263.

(26) Incomplete excitation: (a) Alemany, L. B.; Steuernagel, S.; Amoureux, J.-P.; Callender, R. L.; Barron, A. K. *Solid State NMR* **1999**, *14*, 1. (b) Amoureux, J.-P.; Pruski, M.; Lang, D. P.; Fernandez, C. *J. Magn. Reson.* **1998**, *131*, 170.

The resulting values of $\delta_{\text{iso}} = 100$ ppm and $\delta_{\text{iso}} = 215$ ppm together with the corresponding quadrupolar coupling constants CQ were used as input parameters for a simulation of the single-pulse ^{27}Al MAS spectra, assuming a CQ > 16 MHz for the third component. The simulation produces the spectra shown as solid lines in Figures 3 and 4.

The narrow signal at 102.7 ppm in the ^{27}Al MAS spectrum of **2** (cf. Figure 4) is due to $\text{AlCl}_3 \cdot \text{THF}$,²⁷ which was found as a byproduct in the synthesis of **2** (cf. below) and is not considered any further in this discussion. The resulting parameters for **1** and **2** in comparison with the results of ab initio calculations are given in Table 3.

The signal with the smallest relative area was assigned to the two para Al atoms Al1 and Al1'. This assignment is supported by the virtual independence of the chemical shift of this resonance on the nature of the halogen atom. The very broad signals at 163 (**2**) and 146 ppm (**1**) were ascribed to the exohedral $\text{AlX}_2 \cdot \text{THF}$ units (Al5). Both, the strong dependence of the chemical shift on the nature of the halogen atom and the extremely large quadrupolar coupling support this assignment. The third component with $\delta_{\text{iso}} = 112$ (**2**) and 116 ppm (**1**) consequently corresponds to the endohedral Al atoms Al2, Al3, and Al4.

The parameters δ_{iso} , CQ, and η for **2b** obtained from ab initio calculations are in pleasing agreement with the measured values of **2**. The shift calculated for Al1 is strongly influenced by the donor. For a donor-free Al1 atom in **2a**, we calculated a strong shift to lower field of ~ 800 ppm, which is in the range of theoretically obtained shifts for "naked" Al atoms in metalloid Al clusters.²⁸ Therefore, Al atoms of this species are already situated in an electronic environment that is close to the environment in the metal ($\delta^{27}\text{Al} = 1639$ ppm²⁹). The metalloid character of Al1 is therefore not very pronounced in **1**, **2**, **3**, and **2a**; however, the 12 Al atoms within the icosahedron are not equivalent.

X-ray Photoelectron Spectroscopy (XPS). XPS experiments were conducted to learn more about the influence of the various electronic sites of the Al atoms in **2**. Depending on the electronic environment, the BE of the Al 2p electron ranges from 72.5 eV in Al metal,³⁰ 74–75.7 eV, for example, in aluminum (hydro)oxides,³¹ to 74.7 eV in AlCl_3 and 76.3 eV in AlF_3 ³² with half-widths (fwhm) below 2.5 eV for the unresolved Al 2p doublet. Therefore, a sufficient differentiation of the Al 2p BE should be possible in subvalent Al compounds. Because XPS examines exclusively layers close to the surface (some nanometers depth), the investigation of these highly temperature and oxidation sensitive compounds had to be taken with utmost care in order to prevent method-induced changes. Preexaminations of the tetrahedral Al^I compound Al_4Cp^*_4 (**4**) (cf. Supporting Information) resulted preliminarily in a single component at 73.1 eV. With increasing time of exposure to the X-ray radiation (several hours), a second, larger doublet was observed to grow in at 75.1 eV, although the compound had been cooled to 78 K. This latter doublet results from a decomposition of **4**, which

(27) Hahn, O. H.; Oldfield, E. *Inorg. Chem.* **1990**, *29*, 3666.

(28) (a) $\{\text{Al}_{14}\text{I}_6(\text{N}[\text{SiMe}_3]_2)_6^{2-}\}$: Köhnlein, H.; Stösser, G.; Baum, E.; Möllhausen, E.; Huniar, U.; Schnöckel, H. *Angew. Chem.* **2000**, *112*, 828, *Angew. Chem., Int. Ed.* **2000**, *39*, 799. (b) $\{\text{Al}_7(\text{N}[\text{SiMe}_3]_2)_6^{2-}\}$: Purath, A.; Köppe, R.; Schnöckel, H. *Angew. Chem.* **1999**, *111*, 3114; *Angew. Chem., Int. Ed.* **1999**, *38*, 2926.

(29) Kellberg, L.; Bildsøe, H.; Jacobsen, H. J. *J. Chem. Soc. Chem. Commun.* **1990**, 1294.

(30) Powell, C. J. *Appl. Surf. Sci.* **1995**, *89*, 141.

(31) Bruns, M.; Schlesinger, R.; Klewe-Nebenius, H.; Becht, R.; Ache, H. J. *Mikrochim. Acta* **1995**, *124*, 73.

(32) McGuire, G. E.; Schweitzer, G. K.; Carlson, T. A. *Inorg. Chem.* **1973**, *12*, 2451.

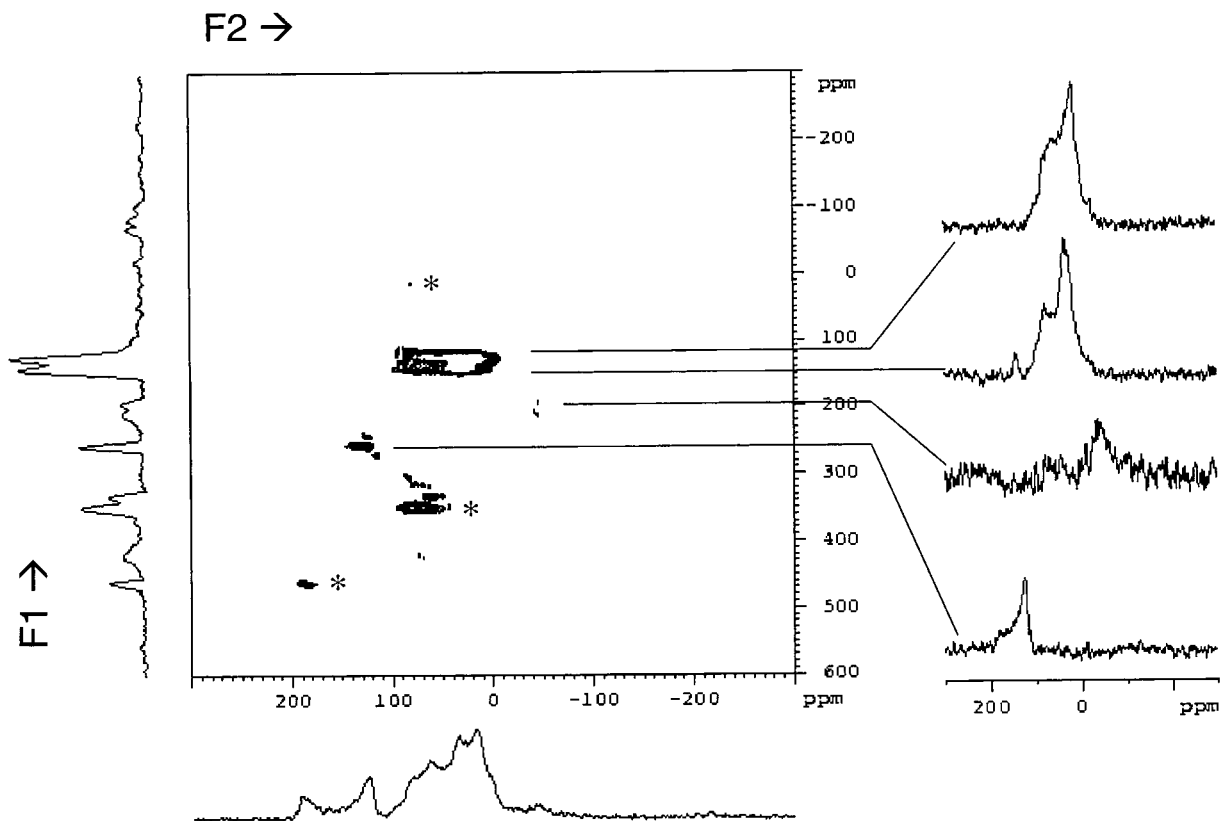


Figure 5. ^{27}Al 3QMAS spectrum of **2**. 1D spectra along the 3Q dimension (F1) and the single quantum dimension (F2) correspond to summations over the peaks in these dimensions. Right side: slices taken at 126, 142, 198, 208, and 258 ppm, respectively.

Table 2. Chemical Shifts in the F1 (MQ) Dimension, Centers of Gravity for the Corresponding Quadrupolar Powder Patterns (Slices Parallel F2), Extracted Isotropic Chemical Shift δ_{iso} , and Second-Order Quadrupolar Effect SOQE

signal	$\delta_{\text{F1}}/\text{ppm}$	$\delta_{\text{F2}}/\text{ppm}$	$\delta_{\text{iso}}/\text{ppm}$	SOQE/MHz
c	258	139	215	11.5
a	126	34	92	10.2
b	142	38	103	11.0
	198			
	208			

Table 3. Results of ^{27}Al NMR Investigations^a

sample	signal	$\delta_{\text{iso}}/\text{ppm}$	CQ/MHz	h	area/%
1	Al1	227	10.9	0.1	7
	Al2-4	116	10.6	0.3	48
	Al5	146	15.8	0.47	45
2	Al1	227	11.2	0.1	10
	Al2-4	112	10.5	0.2	40
	Al5	163	16.5	0.5	50
2b	Al1	228	15	0.01	9
	Al2-4	107	11	0.26	45.5
	Al5	155	19	0.51	45.5

^a Parameters for **1** and **2** obtained from the simulation of the single-pulse spectra and parameters for **2b** obtained from ab initio calculations.

is the topic of further research. However, the signal at 73.1 eV can be assigned to the formally monovalent Al atoms of the Al_4 -polyhedron.

Therefore, **2** was measured quickly by short scanning times for the Al 2p photoelectrons (15 min) in order to reduce decomposition of the sample. The measured XPS spectrum including a peak fit is depicted in Figure 6. The multiplet that can be fitted with three Gaussian peaks centered at 72.6 (9.5%), 74.9 (45.0%), and 76.7 eV (45.5%).

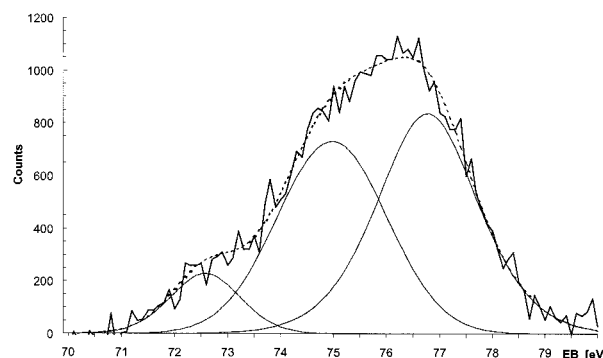


Figure 6. Al 2p BE of **2** resulting from XPS measurement. Gray zigzag line, experimental spectrum; the dotted line corresponds to a simulation of the spectrum assuming three components (below the spectrum).

In accordance to the results of the ^{27}Al NMR investigation, we thus can differentiate three species of Al atoms.³³ The component with the lowest energy, at 72.6 eV, was assigned to

(33) The BE difference between Al1 and Al2-4 is not too surprising since they are not chemically equivalent. This can already be deduced from the molecular structure, where we find a compressed icosahedron resulting from different Al atom radii. Whereas the Al2-4 atoms are completely surrounded by other (electron-deficient) Al atoms, the Al1 atoms are coordinated by the Lewis base THF providing two electrons in accordance with Wade's rules. The influence of the different chemical environment becomes obvious in the case of the ^{27}Al NMR experiments (also supported by quantum chemical calculations). This would not be the case for symmetrical (but always negatively charged) icosahedra like $\text{B}_{12}\text{H}_{12}^{2-}$. To our knowledge, there is only one other example for a neutral molecule with icosahedral structure: 1,12-(SMe₂)₂B₁₂H₁₀ (Hamilton, E. J. M.; Jordan, G. T.; Meyers, E. A.; Shore, S. G. *Inorg. Chem.* **1996**, *35*, 5335.) (two thioether donor molecules!). Unfortunately, there are no BEs known for this compound. A comparison with other "like atoms in a metal-metal bonded cluster" (e.g., the *metalloid* Al clusters) is unfavorable due to a different bonding situation.

the two Al1 atoms of the icosahedron and is close to the BE of elemental aluminum (72.5 eV). The 10 remaining Al atoms of the icosahedron (Al2–4—which are exclusively surrounded by Al atoms but not donor-stabilized) were assigned to the BE at 74.9 eV. Unlike the Al atoms of **4**, this shift to a higher BE points to a lack of electrons in the halide compound **2**. This is also supported by the short Al–Al distance between Al2–4 and the electron-deficient exohedral AlX₂·L fragments surrounding the Al₁₂ polyhedron ($d_{\text{Al4–Al5}} = 2.55 \text{ \AA}$; comparable to L·X₂Al–AlX₂·L compounds^{2a}). The BE for the 10 AlCl₂·L ligands (Al5) of 76.7 eV is positioned above the usual value for trichlorides, and also in this case, a general electron deficiency in **2** can be assumed.

To verify the measured binding energies theoretically, we calculated the energy of an “Al 2p electron hole position” in the cationic **2b** by single-point calculations based on the geometry optimized by DFT methods. This can be easily done by removing one electron from the MOs of the Al₂₂ cluster hosting the Al 2p electrons with regard to their energy (66 2p electrons with slightly varying energy). If the electron with the lowest energy respective to the one with the highest energy is removed from this MO crowd, these two calculated MO energies will thus represent the limits of the values to be expected of the measurement. These calculated binding energies amount to 71.9 and 79.1 eV, respectively. Therefore, the wide range of the experimentally determined BE for the Al 2p electrons is supported by the calculated values. This range of Al 2p BEs confirms our interpretation of **1**, **2**, and **3** to be a trapped molecular product of disproportionation of aluminum(I) halides.

To quantitatively confirm the measured XPS spectrum, more detailed calculations of the corresponding MO energies are necessary and currently on the way. First results indicate a lower BE for Al2–4 than for Al1 and Al1', which is in accordance with the results of the population analysis of **2b**. We found Mullikan charges of +0.5 for Al1, –0.6 for Al2–4, and +1.2 for Al5. Therefore, the possibility that the interpretation of the experimental XPS spectrum of **2** is incomplete due to method-induced impurities cannot be excluded.

Oxidation States/Byproducts. In a formal consideration of the oxidation states of the Al atoms in **1**, **2**, and **3**, the oxidation state is 0 for all 12 atoms of the icosahedron and +2 for the 10 remaining atoms (resulting in an averaged oxidation state of 0.91). Regarding the disproportionation of 24 AlX·L, which would thermodynamically lead to 16 Al and 8 AlX₃·L, these Al₁₂[AlX₂·L]₁₀·2L species **1**, **2**, and **3** can thus be considered as mixed-valent intermediates or “internal disproportionation products” formed by formal elimination of Al₂X₄·2L.

In this case, the first *halogen-deficient* triel subhalides (E_nX_{n–2} type) were isolated during the disproportionation of EX solutions, and therefore, *halogen-rich* byproducts, e.g., of the E_nX_{n+2}-type, have to be formed as well. Thus, in the experiments, the well-known species AlCl₃·THF in the synthesis of **2** and the remarkable compound Al₃Br₇·5THF in the synthesis of **1**^{3c} were also structurally characterized.

Existence of a New Elemental Modification of Al? Because all the Al–Al bonds of **1**, **2**, and **3** are present inside the Al₂₂ cluster core (formally 10 exohedral 2e[–]–2c bonds and 13 binding MOs in the icosahedron) and all the Al–X bonds are outside this cluster core, the molecules **1**, **2**, and **3** represent already *intramolecular* disproportionation products. Thus, the cluster interior can be considered as an intermediate on the way to the element formation. At first glance, it is not obvious that **1**, **2**, and **3** are real intermediates on the way to *aluminum metal* (fcc structure), considering their polyhedral structure. Although

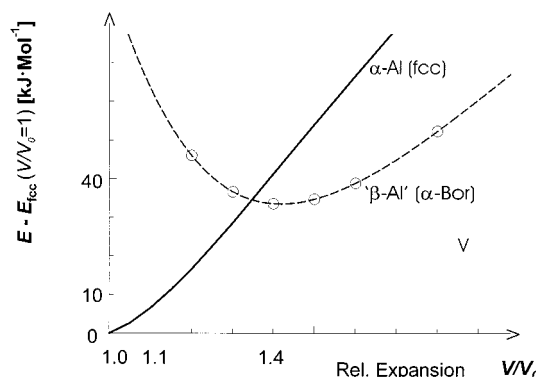


Figure 7. Structural competition between the fcc and α -B type for aluminum during expansion (ab initio full-potential calculations).

the binding properties in these compounds³⁴ are in agreement with Wade’s rules,³⁵ in boron chemistry, no comparable molecular compound with exohedral B–B bonds has been found so far. The latter, however, can be found in the elemental modifications of boron all of which consist of icosahedral units and can as well be described by Wade’s concept.

These results leave the theoretical possibility of a second elemental modification of Al which consists of Al₁₂ icosahedral entities. The simplest structure among the boron modifications is that of α -rhombohedral boron, where B₁₂ icosahedra are arranged as in a cubic close packing of spheres. Within the close-packed layers, icosahedra are connected by 2e[–]–3c bonds (yielding a 5 + 2 coordination of half of the icosahedra forming atoms) whereas icosahedra between layers are terminally linked by 2e[–]–2c bonds resulting in 5 + 1 coordinated atoms. We investigated the structural competition between the fcc and α -B type for Al by means of ab initio full-potential calculations with the results depicted in Figure 7.

At a volume corresponding to that of the experimental (fcc) ground-state modification (V_0), the interatomic Al–Al distances in the open-packed α -B structure get very short and the structure is considerably less stable (by more than 80 kJ·mol^{–1}) than the fcc close packing. However, upon relaxation of the volume, the α -B structure is rapidly stabilized. The optimum volume is slightly above $V/V_0 = 1.4$, corresponding to an expansion of 40% with respect to the ground-state volume. At this volume, the average distances within the Al icosahedra are 2.64 Å, which compares quite well to the range of distances found within the icosahedra of **1**, **2**, and **3**. Additionally, the energy difference has decreased to $\sim 33 \text{ kJ}\cdot\text{mol}^{-1}$ with respect to fcc Al at its ground-state volume.³⁶

Interestingly, the optimization of the interatomic distances of Al in the open-packed α -B structure leads to an atomic volume that corresponds to the condition of expansion. Al in the α -B structure is formally an “expanded metal”! From a theoretical point of view, there is no conceptual difficulty with a state of expansion; it is simply the negative direction on the pressure axis. Naturally, under expansion, a close-packed structure is destabilized and transitions to open-packed structures

(34) Owing to the coordinated donor molecules, both “naked” para Al atoms of the icosahedron (Al1, Al1') can each provide the polyhedral framework with three electrons, whereas the remaining 10 icosahedron Al atoms (Al2–4) can only each provide two electrons due to their bond to the AlX₂ groups. This results in 26 (= 2n + 2 with n = 12) framework electrons for the *closo*-Al₁₂-polyhedron (icosahedron).

(35) Wade, K. *Adv. Inorg. Radiochem.* **1976**, *18*, 1.

(36) These E/V values were obtained from just a volume relaxation of Al in the α -B structure. A complete relaxation of this structure, including the *c/a* ratio and the atomic parameters, results in an even lower value for the optimum volume ($V/V_0 = 1.3$) and the energy difference ($\sim 20 \text{ kJ}\cdot\text{mol}^{-1}$) with respect to fcc Al.

occur. For Al in particular at an expansion $V/V_0 = 1.4$, the interatomic distances in the fcc structure are increased from 2.86 to 3.2 Å and the close-packed structure is by more than 10 $\text{kJ}\cdot\text{mol}^{-1}$ less stable than the open-packed α -B structure. We have found that the idea of computationally expanding metals gives valuable insights into electronic structure relationships^{37a,b} and complements nicely the traditional studies of structural stability as a function of compression.^{37c}

As for elemental high-pressure modifications, an expanded modification is thermodynamically unstable at ambient conditions ($V/V_0 = 1$) and will transform (collapse) to the ground-state structure. However, many high-pressure \rightarrow low-pressure phase transitions are not reversible and the element remains in the metastable high-pressure modification when pressure is released. The most prominent example is the high-pressure modification of carbon (diamond). The same can hold for a hypothetical " β -Al" with the α -B structure (or with any icosahedra-based structure) once it has been synthesized. The disproportionation of Al^I compounds leading to the formation of Al₁₂ icosahedral entities can indeed provide a route for the synthesis of an expanded elemental Al modification. In the first place, the neutral cluster compounds **1**, **2**, and **3** might represent an intermediate for a further reaction where terminally bonded Al^{II} atoms are used to build up a second shell of Al₁₂ entities. Second, if "naked" Al₁₂ icosahedra are formed during the disproportionation process, these units may arrange directly to a three-dimensional structure.

The isolation of larger, metal-rich aluminum subhalides as metastable intermediates (e.g., linked icosahedra) would be a further step in understanding the mechanism and kinetic situation of the disproportionation process. Furthermore, the thermodynamic situation of the disproportionation is of great interest, and this can be investigated by analyzing the relative energies. For this purpose, we calculated the model system **2a**(s) + Al₂Cl₄·2H₂O(s) in relation to the educts (24 AlCl_(g) + 12 H₂O(g)) and the thermodynamically most stable end products (16 Al(s) + 4 AlCl₃·H₂O(s) + 4 AlCl₃·2H₂O(s)). The energy diagram is depicted in Figure 8 and shows that already 81% of the disproportionation energy is liberated when the gaseous educts form solid **2a**.³⁸ With a value of $-740 \text{ kJ}\cdot\text{mol}^{-1}$, the hypothetical condensation of the Al₁₂ icosahedra of **2a** to " β -Al(s)" is exothermic. In terms of thermodynamics, we therefore cannot exclude the possibility of an experimental way to such a previously unknown elemental structure of aluminum.

Conclusion

The formation of elemental aluminum by disproportionation of the stoichiometric Al_nX_n compounds (e.g., cyclic Al₄X₄·4L species) proceeds via halogen-deficient intermediates. The only intermediates isolated so far are **1**, **2**, and **3**, which are E_nX_{n-2}-type species (X = Cl were presented here). Unlike the Al_nX_n

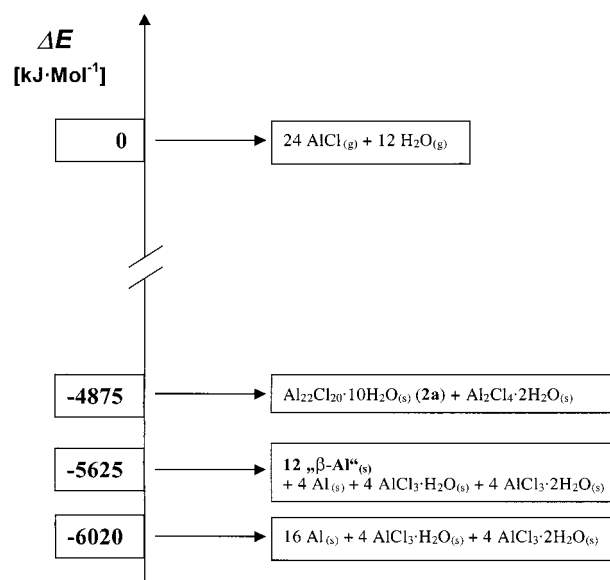


Figure 8. Energetic situation of **2a** and β -Al with respect to the monohalide educt and the thermodynamic end product of metallic α -Al and donor-stabilized trihalides. The hypothetical β -Al could be formed by the disproportionation of **1**, **2**, and **3**.

compounds with $2n$ electrons for $2e^- - 2c$ bonds, which form ring structures, the E_nX_{n-2} compounds such as **1**, **2**, and **3** have $2n + 2$ electrons for the Al cluster core, so that in agreement with Wade's rules, *closo* polyhedral clusters with multiple center bonds are formed. This leads to increased Al–Al distances and a higher coordination number (CN) (within the icosahedron CN = 5–6 with $d_{\text{Al-Al}} = 2.70 \text{ \AA}$ instead of 2.597–2.653 Å in ring compounds). The various substituents (L and AlX₂·L) in **1**, **2**, and **3**, however, cause a distortion of the icosahedron in the direction of a bicapped pentagonal antiprism: This provides different electronic sites for the Al atoms of the icosahedra which can be specified experimentally and by ab initio calculations.

Correspondingly, during further reduction in the direction of the metal, $2n + 4$ electrons for the Al cluster core ($n + 2$ binding MOs) should result in a Al_nX_{n-2}²⁻-type species (similar to Al_nX_{n-4}, as X⁻ can here be considered as a donor). The partially substituted subhalide Al₁₄I₆R₆^{2- 28a} (R = NSi[Me₃]₂) can be regarded as a representative of this species. However, the Al cluster core is not at all a *nido* Wade cluster but an extremely shortened bicapped hexagonal antiprism with an Al–Al distance of 2.73 Å between the capping Al atoms (with CN = 7) and can be derived from the metal structure. Being a derivative of the Al_nX_{n-4}-type species, Al₁₂R₈^{- 39a} has an additional electron and exhibits a section of the metal structure as well as the center of the largest Al cluster (Al₇₇R₂₀²⁻ as a derivative of the Al_nX_{n-59}-type species with a CN up to 12).^{39b}

Unlike boron cluster compounds, which avoid "compact clusters" (in the sense of a fcc section) with a maximum CN (as, for example, in the *conjuncto* borane B₂₀H₁₆,⁴⁰ a formal

(37) (a) Söderlind, P.; Eriksson, O.; Wills, J. M.; Boring, A. M. *Nature* **1999**, *374*, 524. (b) Häussermann, U.; Simak, S. I., submitted to *Chem. Eur. J.* (c) Simak, S. I.; Häussermann, U.; Ahuja, R.; Johansson, B., to be published.

(38) Regarding sublimation enthalpies (H_{subl}) of the products, this calculation has been corrected after the first coarse approximation described in ref 7. Due to the high molecular mass M_r of **2a**, H_{subl} can be approximated with an empiric formula ($H_{\text{subl}} = 0.254M_r - 23.3 = 344 \text{ kJ}\cdot\text{mol}^{-1}$).⁴² For the donor-stabilized aluminum halides, $H_{\text{subl}} = 121 \text{ kJ}\cdot\text{mol}^{-1}$ is assumed corresponding to the literature data of donor-free AlCl₃ as well as of donor-stabilized AlCl₃·NaCl.⁴³ The relative energies of all gaseous molecular compounds were calculated with DFT methods (cf. ref 13). Due to the arithmetically calculated approximations and the cross-linking of the calculated data with the experimentally determined H_{subl} of aluminum (accuracy, $\pm 5 \text{ kJ}\cdot\text{mol}^{-1}$),⁴² more precise quantification and interpretations are not possible.

(39) (a) {Al₁₂(N[SiMe₃]₂)₈⁻}: Purath, A.; Schnöckel, H. *Chem. Commun.* **1999**, 193. (b) Ecker, A.; Weckert, E.; Schnöckel, H. *Nature* **1997**, *387*, 379.

(40) Dobrott, R. D.; Friedman, L. B.; Libscomb, W. N. *J. Chem. Phys.* **1964**, *40*, 866.

(41) (a) Kleier, D. A.; Bicerano, J.; Libscomb, W. N. *Inorg. Chem.* **1980**, *19*, 216. (b) Solntsev, K. A.; Mebel, A. M.; Votnova, N. A.; Kuznetsov, N. T.; Charkin, O. P. *Sov. J. Coord. Chem.* **1992**, *18*, 296; *Koord. Khim.* **1992**, *18*, 340.

(42) Krossing, I. *Chem. Eur. J.* **2001**, *7*, 490.

(43) Lide, D. R., Ed. *J. Phys. Chem. Ref. Data*, Am. Chem. Soc., & Am. Inst. Phys.: New York, 1985; Vol. 14, Suppl. 1.

E_nX_{n-4} -type species), the cluster compounds of aluminum show a strong tendency to form such *metalloid* clusters with a high CN, i.e., sections of the fcc packing.

Considering this inclination, it is surprising, but not unlikely according to the results presented here, that a " β -Al" with a structure analogous to that of boron could be accessible by disproportionation. For this purpose, an absolute prerequisite is the formation of sufficiently large ("expanded") intermediates with an icosahedral Al frame and suitable weakly bonded ligands (L and $AlX_2 \cdot L$) as in the case of **1**, **2**, and **3**.

Acknowledgment. We thank Dr. Dr. H.-J. Himmel and Dr. I. Krossing for helpful discussions.

Supporting Information Available: An X-ray crystallographic file in CIF format for the structure determination of $Al_{22}Cl_{20} \cdot 12THF$ (**2**) and $Al_{22}Cl_{20} \cdot 12THP$ (**3**) as well as XPS spectra for $Al_4Cp^*_4$ (**4**) have been deposited at the database of the American Chemical Society. This material is available free of charge via the Internet at <http://pubs.acs.org>.

JA004022X